Adaptive Bus-Impedance-Damping Control of Multi-Converter System Applying Bidirectional Converters

Roosa-Maria Sallinen, *Student Member, IEEE,* Tomi Roinila, *Member, IEEE*

***Abstract*—Modern dc-power-distribution systems utilizing energy storages are often dependent on the operation of bidirectional power-electronics converters. Such distribution systems typically consist of several feedback-controlled converters prone to experience stability issues due to cross-effects among the different converters. Studies have presented adaptive control-based techniques to prevent such stability issues, but most studies have not fully considered their implementation on a bidirectional converter. The system dynamics may vary significantly depending on the operating point and particularly the direction of the bidirectional power flow. Therefore, specific care should be taken in the design of the adaptive stabilizing control to guarantee that the system's regular operation is not impeded when the stabilization is implemented on a bidirectional converter. This paper proposes a procedure to implement an adaptive stabilizing control method on a bidirectional converter with minimal changes to the regular controller. We add an adaptive resonance term to the bidirectional converter's voltage controller that enhances stability and damping around the identified resonance frequency without impeding the converter's regular operation. The resonance term is adjusted periodically based on online impedance measurements and the chosen design criteria. As a result, the controller can dampen resonances and prevent adverse impedance-based interaction. Experimental measurements based on a multi-converter setup demonstrate the effectiveness of the proposed methods.**

***Index Terms*—adaptive stabilization, dc power systems, resonance-based controller, bidirectional converter, multi-converter system**

I. Introduction

BATTERY energy storage systems (BESSs) play an increasingly important role in many power-distribution systems, such as dc microgrids [2], electric ships [3], and electric aircraft [4]. The operation of these systems typically relies on a bidirectional power-electronics converter, which enables the bidirectional power flow and controls the charge and discharge processes of the energy storage. For such modern power-distribution systems, a dual active bridge (DAB) converter has gained prominence due to its flexible power flow control, zero voltage-switching, high efficiency, galvanic isolation, and modular structure [5]–[7].

Typically, the bidirectional converter is a part of a more complicated multi-converter system in which several converters are connected to a common dc bus, as shown in Fig. 1.

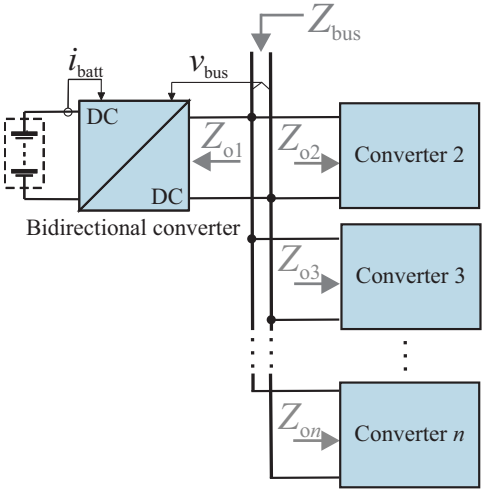

Fig. 1. Multi-converter system with a bidirectional converter.

Such a multi-converter system may experience performance degradation due to impedance interactions between different converters even though the converters may operate well in a standalone mode. The controller of each converter tracks either a voltage, current, or power reference. The high control bandwidth of the load converters introduces a negative incremental impedance at the point of coupling with the dc bus. These load converters act as constant power loads (CPLs). The negative incremental impedance of CPLs has a destabilizing effect on the system [8] and is the main reason for interaction dynamics in dc multi-converter systems [9], [10].

One way of avoiding impedance-based system performance degradation caused by the CPLs is to add passive/active circuit components to the existing system [9], [11]. However, the addition of new components can increase the cost and size of the overall system and slow down the voltage response [12]. Therefore, a more attractive solution is to modify the feedback loops of the individual converters based on system stability assessment [13]–[15].

Considering the stability assessment of a multi-converter system, traditional methods may not be effective with systems including bidirectional converters and varying control structures. Such methods are typically based on minor-loop gain (MLG), which is the ratio between the source subsystem output impedance and the load subsystem input impedance. Examples of such stability assessment methods include the Middlebrook criterion [16] and gain-margin and phase-margin

A preliminary version of the present paper was presented at the IEEE Workshop on Control and Modeling for Power Electronics (COMPEL) 2020, see [1].

R.-M. Sallinen and T. Roinila are with the Faculty of Information Technology and Communication Sciences, Tampere University, 33101 Tampere, Finland (e-mail: roosa.sallinen@tuni.fi, tomi.roinila@tuni.fi).

criterion [17]. These MLG-based methods are not directly applicable to systems with bidirectional power flow because they require the subsystems and system grouping to have specific definitions and formulas [18]. A refined approach for analyzing the stability of a multi-converter system is to apply the MLG by characterizing the converters based on their role in contributing to the current and voltage control rather than assigning them as load and source converters [19]. However, because the control roles may change based on the application operating modes, this method may not be straightforward for all multi-converter systems.

Recent studies have presented passivity-based stability analysis [18], which provides an alternative approach for the stability assessment. This analysis is based on the system bus impedance, rather than the multi-converter system in MLG. The bus impedance represents the total impedance of all the bus-connected subsystems. As the passivity-based method only requires bus-impedance identification, the method is independent of the power-flow directions, the converter operating modes, and the system grouping. This makes the method especially suitable for the stability assessment of multi-converter systems with bidirectional power flow.

The stability enhancement of CPL-affected multi-converter systems on bidirectional converters is still an important problem where different approaches can be useful. Most stabilizing control designs in the literature focus on either the load- or the source-side converters rather than on bidirectional converters; These methods reshape either the output admittance of the CPL [10], [12], [20] or the output admittance of a source converter [21]–[24]. Thus, these methods may not directly apply when implementing a stabilizing controller on a bidirectional converter. Stabilizing control designs for bidirectional converters were presented in [9], [25]–[27]. However, these methods might not be suitable for all applications, as they utilize specific control methods (e.g., semidefinite programming [9]) or are mainly focused on droop-controlled inverters [25]–[27]. Moreover, multi-converter systems can benefit the most from adaptive, nonparametric stabilizing methods that do not require detailed information about the system variables. Such a method was used in [1], where a bus impedance-based stabilizing controller was extended to bidirectional converters, but no experimental results were used to validate the study.

This paper proposes a general, adaptive, nonparametric stabilizing control design method for bidirectional converters in multi-converter systems. This method assesses the multi-converter system stability through bus-impedance identification, and then optimizes the stabilizing controller to dampen resonances within the allowable frequency range. The bus-impedance identification utilizes the existing converters of the system, and employs measurements of the bus-side voltage and currents of each converter. Based on the identification, the stabilizing controller alters the bidirectional converter impedance to provide the desired level of damping for the identified bus impedance in both load- and source-operation modes. Since the stabilizing controller adapts to transitions in the bus impedance, the variations in the operating modes do not degrade the performance. However, owing to the presented design criteria, the stabilizing controller only functions in such a way that the resonance is within the allowable frequency range. This is important because the converter dynamics, such as the current control bandwidth and poles/zeros, limit the available stabilizing controller bandwidth. Therefore, the stabilizing controller does not interfere with the regular controller operation in a degrading manner. The controller scheme is validated with experimental results on a multi-converter system with a DAB converter and two inverters.

The remainder of this paper is organized as follows. Section II presents the bus-impedance-based stability and performance analysis of multi-converter systems. Section III uses this performance assessment to facilitate a resonance-damping control method for adaptive bus-voltage-damping stabilization and describes the identification of bus impedance and the resonance-damping control parameters, as well as the effect of the resonance-damping control on the voltage controller. In Section IV, experimental results validate the effectiveness of the resonance controller on a bidirectional converter operating both as a load and as a source. Conclusions are drawn in Section V.

II. Bus Impedance in Stability Analysis of Multi-Converter Systems

Consider the multi-converter system in Fig. 1; for a multi-converter system of N bus-connected converters, the system's bus impedance (i.e., single-port impedance) $Z_{\rm bus}$ can be given as a parallel connection of the bus-connected impedances, i.e. [28]

$$Z_{\rm bus}(s) = \frac{1}{Z_{\rm o1}^{-1} + Z_{\rm o2}^{-1} + ... + Z_{\rm oN}^{-1}}, \tag{1}$$

where N impedances are identified at the bus-side of the corresponding subsystem (denoted by subscript o in Fig. 1), and the positive signs for the currents correspond to the direction into the converter from the common dc bus. The interconnected multi-converter system can be shown to be passive if the following requirements are met [28].

1) $Z_{\rm bus}(s)$ does not have right half plane (RHP) poles
2) $\mathrm{Re}\{Z_{\rm bus}(j\omega)\} \geq 0, \forall \omega > 0$

Passivity is a sufficient but not a necessary condition for stability. Additional concepts are required to assess other performance metrics (e.g., the level of damping), such as the allowable impedance region (AIR) introduced in [29]. Whereas passivity limits the bus impedance to the RHP, the AIR is defined as a semicircle within the RHP and its radius relates to the chosen attenuation level.

In the case of adverse impedance-based interaction, the bus impedance is typically characterized by a single prominent resonance peak [29]. In such a case, the bus impedance can be expressed as

$$Z_{\rm bus}(j\omega) = Z_{\rm o-bus}\frac{s\omega_{\rm o}}{s^2 + s\omega_{\rm o}/Q_{\rm bus} + \omega_{\rm o}^2}, \tag{2}$$

where $Z_{\rm o-bus}$ is the characteristic impedance, $\omega_{\rm o}$ is the resonance frequency, and the quality factor $Q_{\rm bus}$ specifies the level of damping. Thus, the bus impedance has a real value at the resonance frequency, $Z_{\rm bus}(j\omega_{\rm o}) = Z_{\rm o-bus}Q_{\rm bus}$. In other words, this value depicts the bus impedance peak magnitude.

To achieve a chosen attenuation, the AIR demands that the bus impedance achieves a specified quality factor, $Q_{\max}$. Therefore, the AIR can be defined in the complex plane as a semicircle with a chosen radius of $Z_{\mathrm{o-bus}}Q_{\max}$. In addition, to simplify the performance analysis, the AIR condition can be normalized by dividing the bus impedance and the AIR radius by the characteristic impedance. This normalization results in a straightforward expression for the AIR with a radius of $Q_{\max}$. Accordingly, the chosen attenuation is achieved if the normalized bus impedance $Z_{\mathrm{bus-N}}(j\omega)$ remains within the specified AIR.

Based on (1), the bus impedance peaks when the parallel sum of the impedances is zero, i.e., the impedances are of similar magnitude but an opposite phase. Concerning the individual converters, the shape of their impedance is strongly affected by their control structure. In the case of current controlling converters, their impedance can be described as a CPL since they have a negative incremental impedance within their feedback control loop bandwidth, i.e., the impedance magnitude is resistive with a -180^o phase. In contrast, the impedance of voltage-controlling converters has a relatively small magnitude except for a resonance peak around the voltage control cross-over frequency. Likewise, droop control has the same characteristics as voltage control except for very low frequencies, in which the impedance magnitude is affected by the droop coefficient [30]. When converters of these different types are used together, the resonance peak in the voltage-controlling converter's impedance may cause the parallel sum of the converter impedances to have equal magnitudes at some frequency. If the impedances' phase difference is around -180^o at that same frequency, the denominator in (1) becomes very small, and the bus impedance exhibits significant resonance. This phenomenon is a typical example of adverse impedance-based interactions of multi-converter systems. Fig. 2 shows an example of a typical bus impedance based on (2) in which resonance occurs at 75 Hz.

Utilizing a virtual impedance is a straightforward way to prevent a resonance caused by impedance-based interactions. Essentially, the resonance in the bus impedance is caused by a resonant pole that occurs close to the voltage control cross-over frequency. The resonance typically occurs at a frequency close to the voltage control loop bandwidth. Thus, a virtual impedance in the voltage controlling converter can be designed to dampen the resonance. Even though the resonant behavior could also be smoothed with, for example, an additional capacitor, an adaptive control-oriented solution can offer a more optimized solution.

III. Impedance-Based Adaptive Stabilizing Control of Bidirectional Converters

In a multi-converter system, one of the converter impedances can be reshaped in such a way that the bus impedance achieves a chosen attenuation level. When performed adaptively, impedance reshaping can prevent impedance-based interactions from degrading the multi-converter system performance. Instead of using additional hardware, impedance reshaping can be carried out by modifying the converter control.

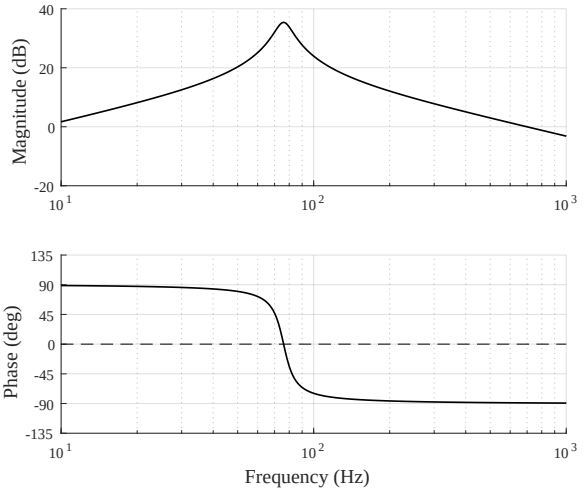

Fig. 2. Frequency response of the bus impedance as given in (2) with $Z_{\mathrm{o-bus}} = 9$, $\omega_{\mathrm{o}} = 477$ rad/s, and $Q_{\mathrm{bus}} = 6.5$.

The control can be designed to offer additional damping to the converter's closed-loop impedance, thus affecting the bus impedance. The range of this damping should be around the identified resonance frequency. For such a stabilizing control design, the following design criteria are required:

- The added virtual impedance itself has a damping level of a chosen quality factor Q_{d}
- The resulting normalized bus impedance $Z_{\mathrm{bus-N}}(j\omega)$ remains within an AIR specified by a chosen quality factor $Q_{\max}$
- At the resonance frequency, the resulting normalized bus impedance $Z_{\mathrm{bus-N}}(j\omega_{\mathrm{o}})$ is limited to remain within an AIR specified by a chosen quality factor $Q_{\max} - K_{\mathrm{m}}$, where K_{m} is an additional margin; The quality factor of the resulting normalized bus impedance $Z_{\mathrm{bus-N}}(j\omega_{\mathrm{o}})$ corresponds to $Q_{\max} - K_{\mathrm{m}}$ at the resonance frequency

Typical ranges for these parameters are $Q_{\max} = 0.7...1$, $K_{\mathrm{m}} = 0...1$, and $Q_{\mathrm{d}} = 0.7...1$. One method of fulfilling the stabilizing control design criteria is to add a specific damping term to the voltage controlling converter's voltage control loop. More specifically, a resonance gain (R-gain) can be added in parallel with the regular voltage controller, given as [31]

$$G_{\mathrm{R}} = \frac{2K_{\mathrm{r}}\omega_{\mathrm{r}}s}{s^2 + 2\omega_{\mathrm{r}}s + \omega_{\mathrm{o}}^2}, \tag{3}$$

where K_{r} determines the damping at the resonance frequency and ω_{r} is the resonance bandwidth. Fig. 3 shows the controller block diagram. The converter operates under cascaded control; the outer voltage loop provides a reference to the inner current loop.

Sufficient values for the R-gain parameters K_{r}, ω_{r}, and ω_{o} can be determined adaptively with online bus impedance identification. First, the resonance frequency ω_{o} can be directly determined from the bus impedance identification. Second, the following design criteria are derived in [24]:

$$K_{\mathrm{r}} = \frac{Q_{\mathrm{d}}}{Z_{\mathrm{o-damp}}}; \omega_{\mathrm{r}} = \frac{\omega_{\mathrm{o}}}{2Q_{\mathrm{d}}}, \tag{4}$$

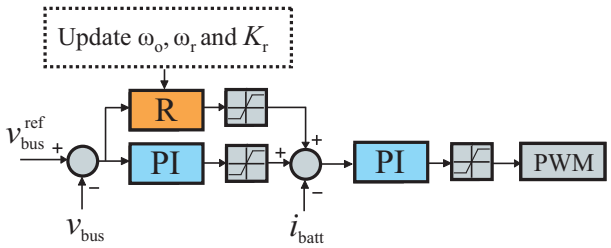

Fig. 3. Block diagram of the converter controller with a resonance term.

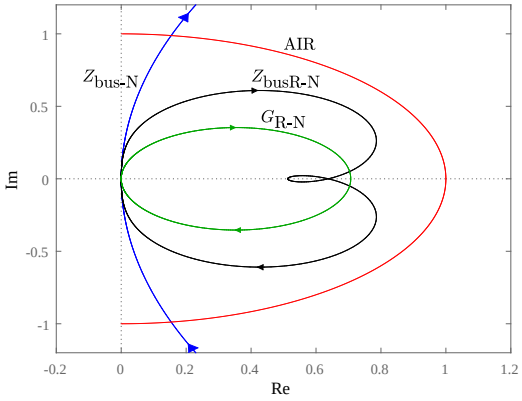

Fig. 4. Normalized bus impedance without R-gain (blue line) and with R-gain (black line), normalized R-gain (green line), and AIR boundary (red line) with $Q_{\rm d}$ = 0.7, $Q_{\rm max}$ = 1, $K_{\rm m}$ = 0.5. Bus impedance as given in (2) with $Z_{\rm o-bus} = 9$, $\omega_{\rm o} = 477$ rad/s, and $Q_{\rm bus} = 6.5$.

where

$$Z_{\rm o-damp} = Z_{\rm o-bus}\frac{Q_{\rm d}Q_{\rm bus}\left(Q_{\rm max}-K_{\rm m}\right)}{Q_{\rm bus}-\left(Q_{\rm max}-K_{\rm m}\right)}. \qquad (5)$$

The adaptive R-gain improves the damping of the bus impedance around the resonance frequency, which improves the multi-converter system's performance and stability. Fig. 4 presents an illustrative example of an R-gain's effect on the normalized bus impedance. The addition of the R-gain decreases the normalized bus impedance quality factor from 6 (out of scale) to within the AIR. Due to the chosen R-gain, the normalized bus impedance attenuation corresponds to $Q_{\rm max} - K_{\rm m}$ at the resonance frequency. In addition, Fig. 4 shows the normalized R-gain (i.e., R-gain multiplied by $Z_{\rm o-damp}$). The virtual impedance itself has damping corresponding to the chosen quality factor $Q_{\rm d}$. Accordingly, all the design criteria have been achieved. Note that if the resonance originates from two CPLs that are coupled through identical resonance frequencies, the resulting virtual impedance cannot prevent the resonance but other methods are required [21].

An R-gain-based stabilizing control is demonstrated in [24] for a source buck converter. In the case of bidirectional converters, the fundamental idea behind the control method is not affected as the bus impedance derivation is independent of the power-flow direction. However, for bidirectional converters, the converter dynamics may change profoundly depending on the operating mode and the power-flow direction. Thus, the stabilizing R-gain control may disturb the regular control

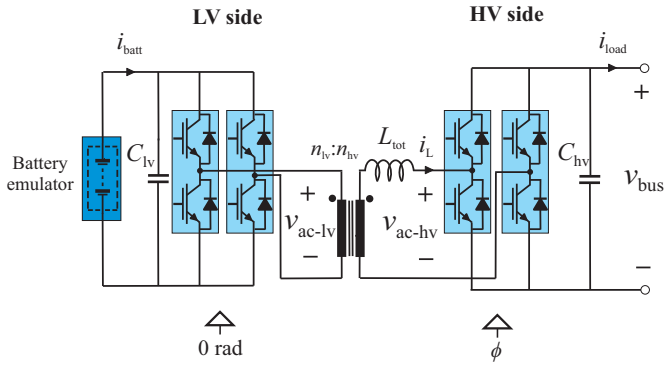

Fig. 5. DAB converter with a battery emulator.

performance and stability if it affects the voltage control loop in a degrading manner. The dynamic changes caused by the change in the operating mode and the power flow direction require further consideration for the successful implementation of the stabilizing controller without regular voltage control degradation or loss of stability.

A. R-Gain Effect on Voltage Control

The nominal voltage control (e.g., PI-based) is typically designed based on the desired phase-margin $\varphi_{\rm m}$ and crossover frequency $f_{\rm c}$. In this work, the stabilizing controller is implemented on a bidirectional DAB dc-dc converter shown in Fig. 5, but the procedure can be utilized in any bidirectional converter topology. The regular current and voltage controllers are based on PI control; the voltage controller is given by $G_{\rm v-PI}(s) = K_{\rm p-v} + K_{\rm i-v}/s$. With the R-gain, the voltage controller becomes $G_{\rm v-PIR}(s) = G_{\rm v-PI}(s) + G_{\rm R}(s)$.

Fig. 6 shows an example of the R-gain effect on the voltage controller gain. The voltage controller gain is presented with and without the R-gain. The R-gain is also shown. The chosen R-gain parameters are $K_{\rm r} = 0.5$, $\omega_{\rm r} = 2\pi 80$ rad/s, and $\omega_{\rm o} = 2\pi 80$ rad/s; the PI-gain parameters are $K_{\rm p-v} = 0.55$ and $K_{\rm i-v} = 704$. As Fig. 6 shows, the R-gain only affects the area around the chosen frequency.

The R-gain effect on the original voltage (PI) controller is small but not necessarily negligible. Since the R-gain increases the voltage control gain within the chosen frequency range, its effect on the phase margin and crossover frequency should be considered to guarantee that the R-gain does not degrade the regular controller performance and stability. The converter dynamics may change profoundly depending on the operating mode and the power flow direction, which should be taken into account in the stabilizing control design and its implementation. For example, if the R-gain bandwidth is too wide, the voltage control crossover frequency may increase beyond the limits of stable operation, which are restricted both by the inner control loop (i.e., the control loops should be decoupled in a cascaded controller) and possible zeros and poles in the converter dynamics. This can be especially important with bidirectional converters, as the system dynamics, specifically, the system poles and zeros, may change profoundly depending on the power direction (e.g., buck vs. boost converter) and thus more easily lead to degraded

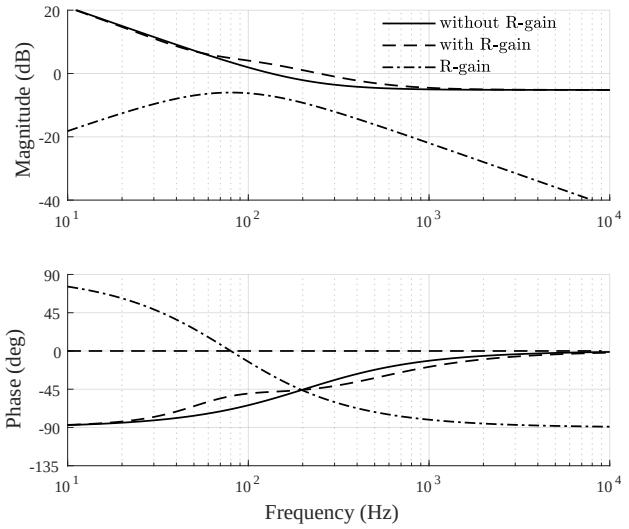

Fig. 6. Frequency response of the voltage controller without (G_{PI}) and with damping ($G_{\mathrm{PI\text{-}R}}$) and the damping R-gain (G_{R}).

control performance. Therefore, further design criteria and implementation methods are required to guarantee the proper operation of the stabilizing controller. As a general guideline, the resonance bandwidth should be limited to

$$\omega_{\mathrm{r-max}} < \frac{2\pi f_{\mathrm{c-innerloop}}^{\mathrm{min}}}{10} < \frac{2\pi f_{\mathrm{sw}}}{10} \tag{6}$$

and

$$\omega_{\mathrm{r-max}} < \frac{2\pi f_{\mathrm{rhp-zero}}}{2}, \tag{7}$$

where f_{sw} is the converter switching frequency, $f_{\mathrm{c-innerloop}}$ is the inner (current) control loop cross-over frequency, and $f_{\mathrm{rhp-zero}}$ is the frequency of a possible right-half-plane zero in the control-to-output voltage transfer function. This transfer function can be given as

$$G_{\mathrm{cv}} = \frac{L_{\mathrm{in}}}{1+L_{\mathrm{in}}}\frac{G_{\mathrm{co-o}}}{G_{\mathrm{ci-o}}}, \tag{8}$$

where L_{in} is the inner loop gain and $G_{\mathrm{co-o}}$ and $G_{\mathrm{ci-o}}$ are the control-to-output voltage and control-to-input current open-loop transfer functions, respectively. Note that since the converter's internal dynamics change based on the operating point and the power direction, these restrictions should be considered in the R-gain stabilizing control design of a bidirectional converter for both power directions. Following these guidelines, the controller can dampen possible resonances in the bus impedance without regular voltage control degradation or loss of stability.

B. Bus Impedance Identification

An adaptive stabilizing controller is desirable in a multi-converter system with varying operating states and conditions. Fortunately, bus impedance identification provides a straightforward method for adjusting the stabilizing control variables because the impedance can be conveniently measured using the converter input and output currents/voltages [32].

Based on (1), the bus-impedance identification requires information about all the interconnected terminal impedances. One method of obtaining the bus impedance is to utilize broadband excitations such as pseudorandom binary sequences (PRBS). While injecting these binary sequences into the converter controllers, the impedances can be identified from the resulting currents and bus voltage with Fourier techniques [28]. The PRBS perturbations are particularly suitable for the identification of power systems, as they have only two signal levels and they have a low crest factor, which means high signal energy in relation to the signal amplitude in the time domain [33]. Note that the PRBS signal's time-domain amplitude and frequency-domain spectrum must be carefully designed for the system under study to guarantee that the system currents and voltage stay within allowable limits and that the perturbations do not excessively degrade the power quality [34].

The impedance identification process should be as fast as possible to enable efficient use of the adaptive stabilizing control so that the system damping can be optimized and a possible distortion can be damped before reaching over-voltage or over-current conditions. For example, unnecessarily low frequencies can be excluded from the PRBS to accelerate the identification process, i.e., frequencies much lower than the voltage control crossover frequency, as specified in (6) and (7). In addition, orthogonal binary sequences can be applied to speed up further the bus impedance identification process and enable simultaneous impedance measurements rather than measuring the required impedances sequentially [35], [36].

One advantage of the impedance-based method is its black box feature; specific knowledge of the system parameters and properties is not needed [37]. Similarly, one of the drawbacks of the impedance-based stability assessment is that it cannot necessarily point the original causes of the resonance without further analysis. Nevertheless, the method offers sufficient information for adapting the virtual impedance according to changes in the multi-converter system so that a possible resonance can be dampened regardless of its root cause.

IV. Experimental results

The proposed method is validated experimentally using a dc multi-converter system consisting of custom-built power converters. The built system and its specifications are shown in Fig. 7, in which a DAB converter is connected to two inverters. The topology of the DAB converter is shown in Fig. 5 and the inverter topologies are typical three-phase, two-level inverters; Their parameters are given in Table I. The DAB converter and Inverter #2 are bidirectional and operate either as a load or as a source depending on the chosen operating point. The DAB converter and Inverter #1 operate under two-loop PI control and the Inverter #2 controls the grid current with PI control. Regular voltage and current measurements are marked in Fig. 7 with black arrows and the orange arrows relate to the current measurements required for the stabilizing R-gain controller. The DAB controller and the Inverter #2 controller are implemented using rapid prototyping controllers by Imperix, whereas the Inverter #1 controller is implemented on dSPACE platform. All the converters are standalone stable, so degradation in the system performance originates from the interactions between the single converters.

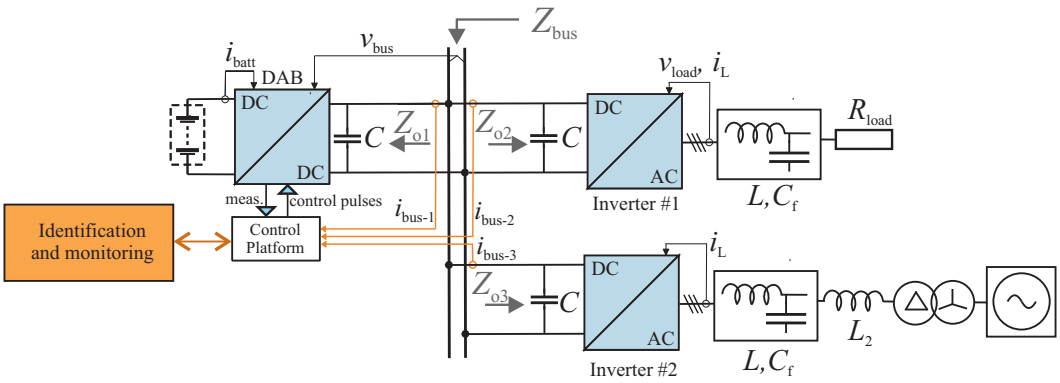

Fig. 7. Laboratory setup for the experimental tests; a multi-converter system consisting of two three-phase inverters and one DAB converter with a battery emulator.

TABLE I
CONVERTER PARAMETERS FOR THE DAB CONVERTER AND THE INVERTERS #1 AND #2 IN FIG. 7.

Parameters	Values (DAB / inv #1 / inv #2)	Description
V_{bus}	400 V	bus voltage
V_{in}	200 V (dc) / 120 V_{rms} (ac) / 120 V_{rms} (ac)	source- or load-side voltage
R_{load}	25 Ω	resistive load of Inverter #1 (star-connection)
f_{sw}	50 kHz / 8 kHz / 20 kHz	switching frequency
C	1.5 mF / 1.5 mF / 1.95 mF	bus-side capacitance
C_{f}	none / 25 μF / 10 μF	inverter ac-side filter capacitance
L_{tot}	300 μH	DAB total inductance
L	none / 2.2 mH / 2.5 mH	inverter ac-side filter inductance
L_2	none / none / 0.6 mH	inverter grid-side filter inductance
$f_{\mathrm{c-c}}$	1 kHz / 500 Hz / 450 Hz	current loop cross-over frequency
$\varphi_{\mathrm{m-c}}$	65^o / 65^o / 60^o	current loop phase margin
$f_{\mathrm{c-v}}$	10 Hz / 6 Hz / none	voltage loop cross-over frequency
$\varphi_{\mathrm{m-v}}$	55^o / 60^o / none	voltage loop phase margin

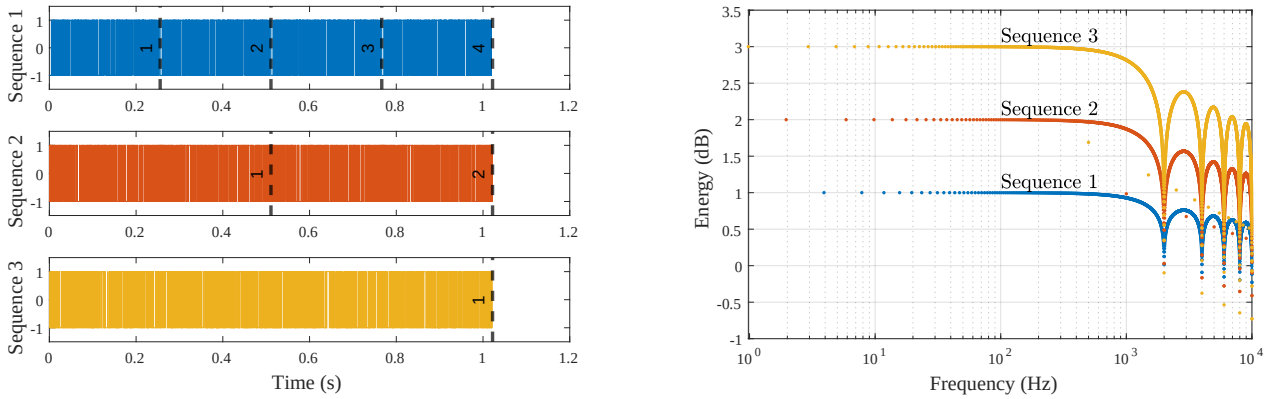

(a) (b)

Fig. 8. MLBS signals used for perturbation for frequency response measurements: (a) in time domain and (b) their energy spectrum.

The perturbation sequences are implemented in all three control platforms. Three orthogonal MLBS sequences are used: Sequence 1 for DAB converter, Sequence 2 for Inverter #1, and Sequence 3 for Inverter #2. Sequence 1 is of length $N = 2^9 - 1$. Since the sequences are orthogonal, the length of Sequence 2 is $2N$, and the length of Sequence 3 is $4N$. Fig. 8 shows the three sequences in both the time and frequency domain. The sequences are generated at $f_{\mathrm{gen}} = 2$ kHz, which provides an 800 Hz bandwidth for the measured frequency responses. The frequency range of interest (i.e., around the voltage control cross-over frequency) is well within the chosen energy spectrum. As demonstrated in Fig. 8, Sequence 3 has a period length of 1.022 s, during which the other sequences are repeated periodically. The actual injection amplitudes are selected such that their values are 5-7 percent of the nominal voltage/current reference values.

The designed perturbations were simultaneously placed on top of the controller reference voltages and/or currents of each converter. The first perturbation was applied with three periods, the second with six periods, and the third with 12

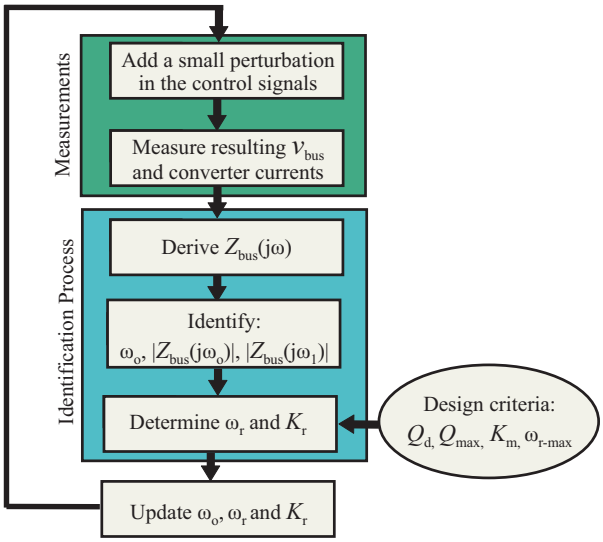

Fig. 9. Flowchart representing the adaptive resonance-damping algorithm with the chosen design criteria.

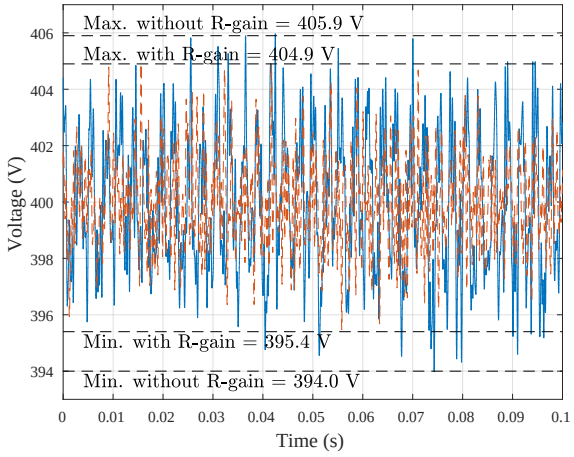

Fig. 10. Low-pass filtered (500 Hz) bus voltage without (blue) and with (orange) damping R-gain while discharging the battery.

periods (because each perturbation length is twice compared to the previous one). The resulting bus voltage and output current of each converter were then measured using a sampling rate of 50 kHz. The measurements were averaged over the applied periods and Fourier transform was used to obtain the output impedances of each converter. The bus impedance was then computed based on (1). After the identification process, the R-gain was added to the DAB controller and its parameters were assigned based on the identified bus impedance and (4) with $Q_{\mathrm{d}} = 0.7$, $Q_{\mathrm{max}} = 1$, and $K_{\mathrm{m}} = 0.4$.

The experiments were conducted at two different operating points: the DAB converter was either feeding the dc bus with 500 W while discharging the battery, or consuming 350 W while charging the battery. This change in the operating point was achieved by changing the Inverter #2 from feeding the grid with 150 W to feeding the dc bus with 700 W. Fig. 9 outlines the bus impedance identification and the controller update process. First, the discharging mode was considered.

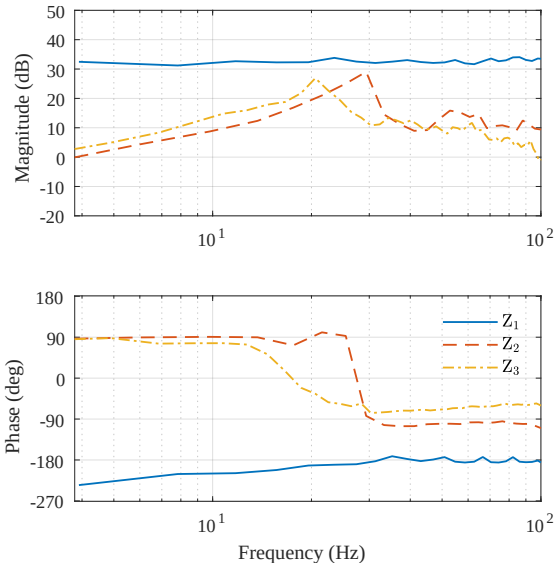

Fig. 11. The identified impedances without damping R-gain while discharging the battery.

The blue line in Fig. 10 shows the bus voltage when the battery is discharging and no R-gain is applied. The minimum (394.0 V) and maximum (405.09 V) values are also marked, meaning a voltage deviation of 2.77 percent. Fig. 11 shows the identified impedances, and the resulting bus impedance is shown in Fig. 12 with a blue line. Without the R-gain, the bus impedance has a magnitude of 37 dB at 21 Hz, highlighted with a marker in Fig. 12. To improve stability, the proposed PI-R controller is activated so that an enhanced damping is achieved around the chosen frequency. Following the aforementioned design procedure and the identified bus impedance, the values of $K_{\mathrm{r}} = 0.17$ and $\omega_{\mathrm{r}} = 18$ Hz are obtained for the R-gain. The resulting bus impedance with the added R-gain is shown in Fig. 12 with a red line. The R-gain increases the bus impedance damping around the identified resonance frequency (21 Hz), lowering it to 11 dB and thus improving the system damping. The resulting bus voltage is shown with the orange line in Fig. 10, and the minimum (395.4 V) and maximum (404.9 V) values are shown resulting in 2.38 percent voltage deviation. Since the voltage variation is lower, the added damping shows an improvement compared to the case without the R-gain.

Next, a similar study is performed while charging the battery. The voltages are comparable to Fig. 10. The identified bus impedance without the R-gain is shown in Fig. 12 with a purple line: without the R-gain, the bus impedance has a magnitude of 23 dB at 13 Hz, highlighted with a marker in the figure. As before, the proposed PI-R controller is activated (now with $K_{\mathrm{r}} = 0.25$, $\omega_{\mathrm{r}} = 7$ Hz) and the resulting bus impedance is shown in Fig. 12 with the yellow line. The R-gain increases the bus impedance damping around 13 Hz, lowering it to 12 dB.

In both the discharging and charging experiments, the damping R-gain controller enhanced the system stability and damping around the identified resonance frequency. The R-gain controllers optimized the identified bus impedances, which were

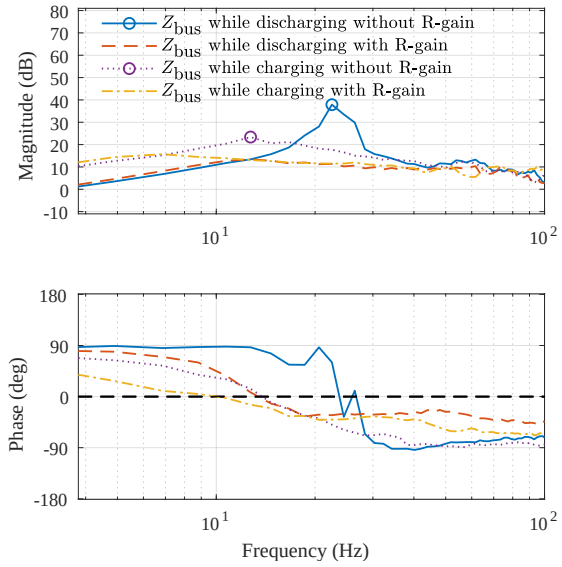

Fig. 12. The identified bus impedances with and without damping R-gain while discharging or charging the battery. Marker highlights the identified resonance.

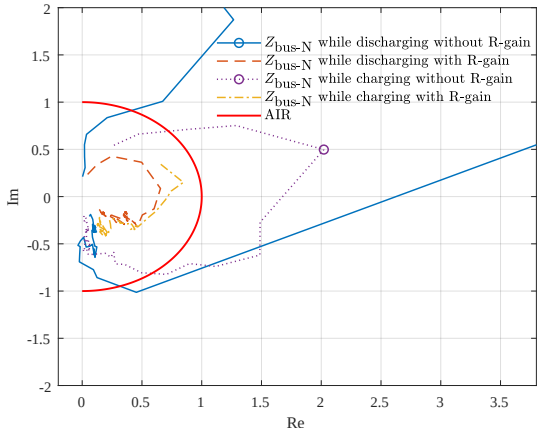

Fig. 13. The Nyquist contour of the normalized bus impedance with and without damping R-gain. AIR boundary indicated with the red line. Marker highlights the identified resonance.

well-stabilized in both charging mode and discharging mode. Fig. 13 presents the corresponding normalized bus impedances in a complex plane. The normalized bus impedances with the R-gain have more damping and are well-confined within the AIR boundary. The Nyquist contour of the R-gain affected normalized bus impedances intersects with the real axis around the requested magnitude, indicating the achievement of the desired damping level. With the R-gain, the system damping is within the desired limits. The experimental results confirm the effectiveness of the proposed adaptive stabilization method in both power directions.

V. Conclusion

This paper has implemented adaptive virtual-impedance-based stabilizing control on a bidirectional dc-dc converter. With the stabilizing resonance-damping control and the provided design guidelines, the bidirectional converter can operate as a virtual impedance that dampens resonances in the bus impedance when required without deteriorating the regular control operation. As a result, the stabilizing control can prevent adverse impedance-based interactions within a multi-converter system and optimize system stability and performance. The stabilizing controller is tuned adaptively based on an online bus impedance identification that estimates the system's stability and performance. The broadband-based identification method is well-suited for adaptive control due to its short measurement cycle. Therefore, the stabilizing control is suitable for multi-converter systems with changing operating states and conditions, such as bidirectional power flow. The analysis and experiments show that the bidirectional converter can efficiently optimize the damping in the bus impedance in both power directions. As a result, the multi-converter system performance is maintained regardless of changes (e.g., in connections or operating modes) and without hardware updates or re-tuning of the regular (such as PI) controller. The resonance-damping control method's simplicity (including bus impedance-based stability assessment and lack of more excessive computations) and basic requirements (such as voltage and current measurements at the bus-side of each converter) mean it can be efficiently embedded in parallel with a regular controller without disturbing its usual operation.

References

[1] R.-M. Sallinen, T. Roinila, and H. Abdollahi, "Stability analysis and adaptive resonance damping of multi-converter system applying bidirectional converter," in *Proc. IEEE Workshop on Control and Modeling for Power Electronics*, 2020, pp. 1–7.

[2] T. K. Roy, M. A. Mahmud, A. M. T. Oo, M. E. Haque, K. M. Muttaqi, and N. Mendis, "Nonlinear adaptive backstepping controller design for islanded dc microgrids," *IEEE Transactions on Industry Applications*, vol. 54, no. 3, pp. 2857–2873, 2018.

[3] Z. Jin, L. Meng, J. M. Guerrero, and R. Han, "Hierarchical control design for a shipboard power system with dc distribution and energy storage aboard future more-electric ships," *IEEE Transactions on Industrial Informatics*, vol. 14, no. 2, pp. 703–714, 2018.

[4] H. Zhang, F. Mollet, C. Saudemont, and B. Robyns, "Experimental validation of energy storage system management strategies for a local dc distribution system of more electric aircraft," *IEEE Transactions on Industrial Electronics*, vol. 57, no. 12, pp. 3905–3916, 2010.

[5] I. Alhurayyis, A. Elkhateb, and J. Morrow, "Isolated and nonisolated dc-to-dc converters for medium-voltage dc networks: A review," *IEEE Journal of Emerging and Selected Topics in Power Electronics*, vol. 9, no. 6, pp. 7486–7500, 2021.

[6] R. De Doncker, D. Divan, and M. Kheraluwala, "A three-phase soft-switched high-power-density dc/dc converter for high-power applications," *IEEE Transactions on Industry Applications*, vol. 27, no. 1, pp. 63–73, 1991.

[7] F. Krismer and J. W. Kolar, "Efficiency-optimized high-current dual active bridge converter for automotive applications," *IEEE Transactions on Industrial Electronics*, vol. 59, no. 7, pp. 2745–2760, 2012.

[8] Xiaogang Feng, Jinjun Liu, and F. C. Lee, "Impedance specifications for stable dc distributed power systems," *IEEE Transactions on Power Electronics*, vol. 17, no. 2, pp. 157–162, 2002.

[9] L. Herrera, W. Zhang, and J. Wang, "Stability analysis and controller design of dc microgrids with constant power loads," *IEEE Transactions on Smart Grid*, vol. 8, no. 2, pp. 881–888, 2017.

[10] X. Lu, K. Sun, J. M. Guerrero, J. C. Vasquez, L. Huang, and J. Wang, "Stability enhancement based on virtual impedance for dc microgrids with constant power loads," *IEEE Transactions on Smart Grid*, vol. 6, no. 6, pp. 2770–2783, 2015.

[11] M. Cespedes, L. Xing, and J. Sun, "Constant-power load system stabilization by passive damping," *IEEE Transactions on Power Electronics*, vol. 26, no. 7, pp. 1832–1836, 2011.

[12] W. Lee and S. Sul, "Dc-link voltage stabilization for reduced dc-link capacitor inverter," *IEEE Transactions on Industry Applications*, vol. 50, no. 1, pp. 404–414, 2014.

[13] S. Fan, F. Wu, and H. Liu, "Unified closed-loop control and parameters design of buck-boost current-fed isolated dc-dc converter with constant power load," *IEEE Journal of Emerging and Selected Topics in Power Electronics*, pp. 1–1, 2021.
[14] W. He and R. Ortega, "Design and implementation of adaptive energy shaping control for dc–dc converters with constant power loads," *IEEE Transactions on Industrial Informatics*, vol. 16, no. 8, pp. 5053–5064, 2020.
[15] X. Zhang, Q.-C. Zhong, and W.-L. Ming, "Stabilization of cascaded dc/dc converters via adaptive series-virtual-impedance control of the load converter," *IEEE Transactions on Power Electronics*, vol. 31, no. 9, pp. 6057–6063, 2016.
[16] R. D. Middlebrook, "Input filter considerations in design and application of switching regulators," in *Conf. Rec. IEEE IAS Annu. Meeting*, 1976, pp. 366–382.
[17] C. Wildrick, F. Lee, B. Cho, and B. Choi, "A method of defining the load impedance specification for a stable distributed power system," *IEEE Transactions on Power Electronics*, vol. 10, no. 3, pp. 280–285, 1995.
[18] A. Riccobono and E. Santi, "Comprehensive review of stability criteria for dc power distribution systems," *IEEE Transactions on Industry Applications*, vol. 50, no. 5, pp. 3525–3535, 2014.
[19] X. Zhang, X. Ruan, and C. K. Tse, "Impedance-based local stability criterion for dc distributed power systems," *IEEE Transactions on Circuits and Systems I: Regular Papers*, vol. 62, no. 3, pp. 916–925, 2015.
[20] B. A. Martinez-Treviño, A. E. Aroudi, A. Cid-Pastor, and L. Martinez-Salamero, "Nonlinear control for output voltage regulation of a boost converter with a constant power load," *IEEE Transactions on Power Electronics*, vol. 34, no. 11, pp. 10 381–10 385, 2019.
[21] M. Wu and D. D. Lu, "A novel stabilization method of lc input filter with constant power loads without load performance compromise in dc microgrids," *IEEE Transactions on Industrial Electronics*, vol. 62, no. 7, pp. 4552–4562, 2015.
[22] S. Liu, P. Su, and L. Zhang, "A virtual negative inductor stabilizing strategy for dc microgrid with constant power loads," *IEEE Access*, vol. 6, pp. 59 728–59 741, 2018.
[23] X. Zhang, Q. Zhong, V. Kadirkamanathan, J. He, and J. Huang, "Source-side series-virtual-impedance control to improve the cascaded system stability and the dynamic performance of its source converter," *IEEE Transactions on Power Electronics*, vol. 34, no. 6, pp. 5854–5866, 2019.
[24] H. Abdollahi, S. Arrua, T. Roinila, and E. Santi, "A novel dc power distribution system stabilization method based on adaptive resonance-enhanced voltage controller," *IEEE Transactions on Industrial Electronics*, vol. 66, no. 7, pp. 5653–5662, 2019.
[25] H. Xiao, A. Luo, Z. Shuai, G. Jin, and Y. Huang, "An improved control method for multiple bidirectional power converters in hybrid ac/dc microgrid," *IEEE Transactions on Smart Grid*, vol. 7, no. 1, pp. 340–347, 2016.
[26] J. He, L. Du, B. Liang, Y. Li, and C. Wang, "A coupled virtual impedance for parallel ac/dc converter based power electronics system," *IEEE Transactions on Smart Grid*, vol. 10, no. 3, pp. 3387–3400, 2019.
[27] P. Yang, M. Yu, Q. Wu, N. Hatziargyriou, Y. Xia, and W. Wei, "Decentralized bidirectional voltage supporting control for multi-mode hybrid ac/dc microgrid," *IEEE Transactions on Smart Grid*, vol. 11, no. 3, pp. 2615–2626, 2020.
[28] A. Riccobono and E. Santi, "A novel passivity-based stability criterion (pbsc) for switching converter dc distribution systems," in *Proc. Annual IEEE Applied Power Electronics Conference and Exposition*, 2012, pp. 2560–2567.
[29] J. Siegers, S. Arrua, and E. Santi, "Stabilizing controller design for multibus mvdc distribution systems using a passivity-based stability criterion and positive feedforward control," *IEEE Journal of Emerging and Selected Topics in Power Electronics*, vol. 5, no. 1, pp. 14–27, 2017.
[30] G. Liu, P. Mattavelli, and S. Saggini, "Design of droop controllers for converters in dc microgrids towards reducing bus capacitance," in *European Conference on Power Electronics and Applications*, 2018, pp. P.1–P.9.
[31] D. N. Zmood and D. G. Holmes, "Stationary frame current regulation of pwm inverters with zero steady-state error," *IEEE Transactions on Power Electronics*, vol. 18, no. 3, pp. 814–822, 2003.
[32] T. Roinila, T. Messo, R. Luhtala, R. Scharrenberg, E. C. W. de Jong, A. Fabian, and Y. Sun, "Hardware-in-the-loop methods for real-time frequency-response measurements of on-board power distribution systems," *IEEE Transactions on Industrial Electronics*, vol. 66, no. 7, pp. 5769–5777, 2019.
[33] A. H. Tan and K. R. Godfrey, *Industrial Process Identification*. Cham, Switzerland: Springer, 2019.
[34] R. Pintelon and J. Schoukens, *System Identification - A Frequency Domain Approach*. New Jersey, US: Institute of Electrical and Electronics Engineers, Inc., 2001.
[35] T. Roinila, H. Abdollahi, S. Arrua, and E. Santi, "Real-time stability analysis and control of multiconverter systems by using mimo-identification techniques," *IEEE Transactions on Power Electronics*, vol. 34, no. 4, pp. 3948–3957, 2019.
[36] T. Roinila, H. Abdollahi, and E. Santi, "Frequency-domain identification based on pseudorandom sequences in analysis and control of dc power distribution systems: A review," *IEEE Transactions on Power Electronics*, vol. 36, no. 4, pp. 3744–3756, 2021.
[37] G. O. Kalcon, G. P. Adam, O. Anaya-Lara, S. Lo, and K. Uhlen, "Small-signal stability analysis of multi-terminal vsc-based dc transmission systems," *IEEE Transactions on Power Systems*, vol. 27, no. 4, pp. 1818–1830, 2012.

Roosa-Maria Sallinen (S'18) received the B.Sc. (Tech.) and M.Sc. (Tech.) degrees in electrical engineering from the Tampere University of Technology, Tampere, Finland, in 2015 and 2017, respectively.

Since 2017, she has been pursuing the Ph.D. degree at the Faculty of Information Technology and Communication Sciences, Tampere University, Tampere, Finland. In 2022, she joined GE Grid Solutions, Tampere, Finland, where she is currently a Lead Control Engineer. Her main research interests include impedance-based interactions in power electronic systems and adaptive stabilization.

Tomi Roinila (M'10) received the M.Sc.(Tech.) and Dr.Tech. degrees in automation and control engineering from Tampere University of Technology, Tampere, Finland, in 2006 and 2010, respectively. He is currently an Associate Professor in Tampere University, Finland.

His main research interests include modeling and control of grid-connected power-electronics systems, analysis of energy-storage systems, and modeling of multi-converter systems.